in vivo *37*: 1486-1497 (2023)
doi:10.21873/invivo.13233

The EGF Motif With CXDXXXXYXCXC Sequence Suppresses Fibrosis in a Mouse Skin Wound Model

HISATAKA KITANO[1*], TOMOMI ISHIKAWA[1*], YOH MASAOKA[2], KAZUHIRO KOMIYAMA[2], MAMIKO TAKAHASHI[2] and CHIAKI HIDAI[3]

[1]*Division of Oral Surgery, Nihon University School of Medicine, Tokyo, Japan;*
[2]*Division of Physiology, Nihon University School of Medicine, Tokyo, Japan;*
[3]*Division of Medical Education, Nihon University School of Medicine, Tokyo, Japan*

Abstract. *Background/Aim: Fibrosis is an essential process for wound healing, but excessive fibrosis, such as keloids and hypertrophic scars, can cause cosmetic and functional problems. These lesions are caused by abnormal deposition and shrinkage of collagen fibers. The light chain of FIX, a plasma protein essential for hemostasis, has the amino acid sequence CXDXXXXYXCXC in the EGF domain. Peptides containing this sequence inhibited stromal growth in a mouse transplant tumor model. In this study, the effect of the FIX light chain on wound healing was studied. Materials and Methods: A full-layer wound was made on the back of each mouse, and cDNA encoding the light chain of mouse FIX (F9-LC) in an expression vector was injected locally once each week using a non-viral vector. Histochemical analysis of the wound was then performed to assess the effects on wound healing. Moreover, the effect of F9-LC on fibroblasts was studied in vitro. Results: Macroscopic observation showed that wounds with forced expression of F9-LC appeared flatter and had fewer wrinkles than control wounds. Tissue collagen staining and immunostaining revealed that administration of F9-LC suppressed collagen 1 and 3 deposition and decreased α–smooth muscle actin expression. Electron microscopy revealed sparse and disorganized collagen fibers in the F9-LC–treated mice. In experiments using fibroblasts, addition of a recombinant protein of the FIX light chain disrupted the typical spindle shape and alignment of fibroblasts. Conclusion: F9-LC is a new candidate for use in treatments to regulate excessive fibrosis and contraction in wound healing.*

Pathological fibrosis is generally a hallmark of advanced stages of disease in many organs, including the liver, kidney, lung, and heart (1). Fibrosis is related to wound healing because of similarities in the underlying processes, the presence of myofibroblasts, and extensive collagen deposition. Fibrosis that produces scarring in the wound healing process can result in the formation of hypertrophic scars and keloids, which can cause significant problems in plastic surgery (2, 3). These pathological changes can occur as a result of a variety of wound types, such as those associated with surgery, piercing, and acne. Hypertrophic scars and keloids sometimes cause pain and itching and can cause abnormal joint mobility depending on the severity and site. Cosmetic problems arising from these scars can cause psychological trauma. Despite considerable effort to elucidate the underlying mechanism and develop therapeutics, hypertrophic scarring and keloids remain clinically problematic.

Typical wound healing processes have been well studied (4, 5). When blood vessels are damaged at the time of injury, platelets and coagulation factors initiate hemostasis (hemostasis phase) (6-8). Inflammatory cells then migrate into the wound area for 3 to 4 days from the time of injury (inflammation phase) (6-8). The subsequent proliferation phase lasts for 3 to 4 weeks (6-8). The proliferation of fibroblasts, epithelial cells, and endothelial cells leads to the formation of granular tissue (6-8). Myofibroblasts contribute to collagen deposition in the proliferation phase (6-8). Finally, regression of scarring can continue for several years (remodeling phase) (6-8). In hypertrophic scarring and keloid formation, massive fibrosis develops along with excessive deposition of extracellular

*These Authors contributed equally to this work.

Correspondence to: Chiaki Hidai, Division of Medical Education, Nihon University School of Medicine, 30-1 Ohyaguchikami-chou, Itabashi-ku, Tokyo 173-8610, Japan. Tel: +81 339728111, Fax: +81 339728810, e-mail: hidai.chiaki@nihon-u.ac.jp

Key Words: EGF motif, CXDXXXXYXCXC, coagulation factor IX, developmental endothelial locus 1, fibrosis.

matrix proteins and mucopolysaccharides (9, 10). The pathogenesis of hypertrophic scarring and keloid formation involves dysregulation of the wound healing process.

Immoderate growth of mesenchymal tissue occurs in cancer as well as abnormal wound healing (11, 12). Cancer tissues generally consist of epithelial cancer cells (parenchyma) and mesenchymal tissue (stroma), both of which grow coordinately and indefinitely. As such, cancer is known as a "wound that never heals". The stroma is essential for parenchymal growth in cancer, as it supplies blood vessels and nutritional support to cancer cells (13). Kitano *et al*. reported that forced expression of a recombinant protein with the third epithelial growth factor (EGF)-like domain (E3) of developmental endothelial locus-1 (Del1), an extracellular matrix protein secreted by endothelial cells, suppressed the growth of explanted squamous cell carcinoma tumors in a mouse model (14-18). The EGF-like domain includes the amino acid sequence CXDXXXXYXCXC, which reportedly induces apoptosis (19). Treatment with EGF-like domain was shown to induce apoptosis in the parenchyma and stroma, resulting in poor stromal development in explanted tumors (14, 15). The similarities between cancer growth and wound healing led us to hypothesize that treatment with EGF domains with a CXDXXXXYXCXC sequence would suppress the growth of mesenchymal tissue in wound healing.

The present study investigated the effect of coagulation factor IX (FIX) light chain (F9-LC) on wound healing using a mouse wound healing model. Vitamin K–dependent coagulation factors, VII, IX, and X, are highly homologous with a similar constitution (20). They are constructed from a few EGF motifs and a proteinase domain. The light chains of these factors contain an EGF motif with a CXDXXXXYXCXC sequence (21). Proteins with the EGF motif are thought to suppress the growth of mesenchymal tissues in wounds. In this study, a cDNA encoding F9-LC was locally injected into induced wounds *via* a non-viral vector; the heavy chain was not employed to avoid the effect of peptidase activity on hemostasis. Forced expression of F9-LC suppressed the deposition of collagen and deformation with wrinkles in the wound. These results indicate that FIX affects fibrosis in wound healing and provide novel insights into potential therapeutics for treating hypertrophic scars and keloids.

Materials and Methods

Reagents. Recombinant fusion proteins were prepared as described previously. Briefly, a cDNA encoding the F9-LC (amino acids 47-191 of mouse FIX) was generated using RT-PCR and then cloned into the AP-tag4 vector (GenHunter, Nashville, TN, USA) for production of AP-tagged FIX as a secreted protein. The AP-tag4 vector was used for control experiments. Plasmids for production of the AP-tagged light chain of FIX (pF9-LC) and AP-tag (control protein) as a secreted protein were transferred into CHO cells to obtain conditioned medium. AP activity was measured by adding 20 μl of conditioned medium. The plate was then heated at 65˚C for 30 min to inactivate endogenous AP, and the enzyme reaction was initiated by adding 200 μl of substrate [1 mg/ml p-nitrophenyl phosphate (Sigma, St. Louis, MO, USA) in 1 mM $MgCl_2$ and 1 M diethanolamine (pH 9.8)] to each well. The absorbance at 405 nm was measured after 30 min.

Mouse Del1 cDNA was obtained as a gift from Dr. Quertermous (Stanford University, Stanford, CA, USA). To generate the plasmids used in the study, a fragment encoding the E3 and C1 sequence (E3C1, amino acids 122-316 of mouse Del1) was amplified using PCR and cloned into the pcDNA3.1D vector (Invitrogen, Carlsbad, CA, USA). An empty pcDNA3.1D vector was used for control experiments.

Animal studies. All animal experiments described in this study were carried out in accordance with both institutional and National Institutes of Health animal care regulations and approved by the institutional ethics committee (AP15M017, AP10M043).

For the wound healing model, ICR mice (5 weeks old, male) were employed. A 1×2 cm full-thickness excisional wound was made on the dorsal skin of each mouse, and the wound was then subcutaneously injected with pF9-LC or pAP, a mock vector. For treatment, 10 μg of DNA was injected into the tumor in 100-μl increments once each week using an *In vivo* Jet-PEI (PolyPlus-transfection; San Marcos, CA, USA). Mice were observed and photographed, and the wounds were measured with a ruler on days 4, 21, 28, and 43. Before taking photographs, the pelage was removed using hair removal cream. The area of the denuded wound was calculated using the following formula: width×length×π/4. For histological examination, mice were sacrificed under deep anesthesia with isoflurane after 43 days of treatment, and the tumors were then harvested, and 5-μm frozen sections were prepared.

Explanted tumor models were generated as described previously (14-18). Briefly, Nu/Nu athymic nude mice were injected subcutaneously in the right flank with squamous cell carcinoma KN (SCCKN) cells. When the tumor volume exceeded 60 mm^3, treatment was initiated with pE3C1 or pcDNA3, a mock vector. For treatment, 10 μg of DNA was injected into the tumor in 100-μl increments once each week using an *in vivo* Jet-PEI (PolyPlus-transfection). For histological analyses, mice were sacrificed under deep anesthesia with isoflurane after 4 weeks of treatment, the tumors were harvested, and 5-μm frozen sections were prepared.

Collagen staining. Collagen staining of frozen section was performed using a collagen stain kit (Collagen Research Center, Tokyo, Japan) according to the manufacturer's protocol. In this method, collagens are stained red, and non-collagen proteins are stained green. Because the pigments can be extracted from stained specimens on glass plates using the extraction solution included in the kit, the relative amounts of collagen and non-collagen proteins can be calculated by measurement of the optical density at 530 nm (OD_{530}) and OD_{605}.

Transmission electron microscopy (TEM). Tissues were initially fixed in 4% paraformaldehyde and then in 2.5% glutaraldehyde in cacodylate buffer (pH 7.4), treated with 1% cacodylate-buffered (0.1

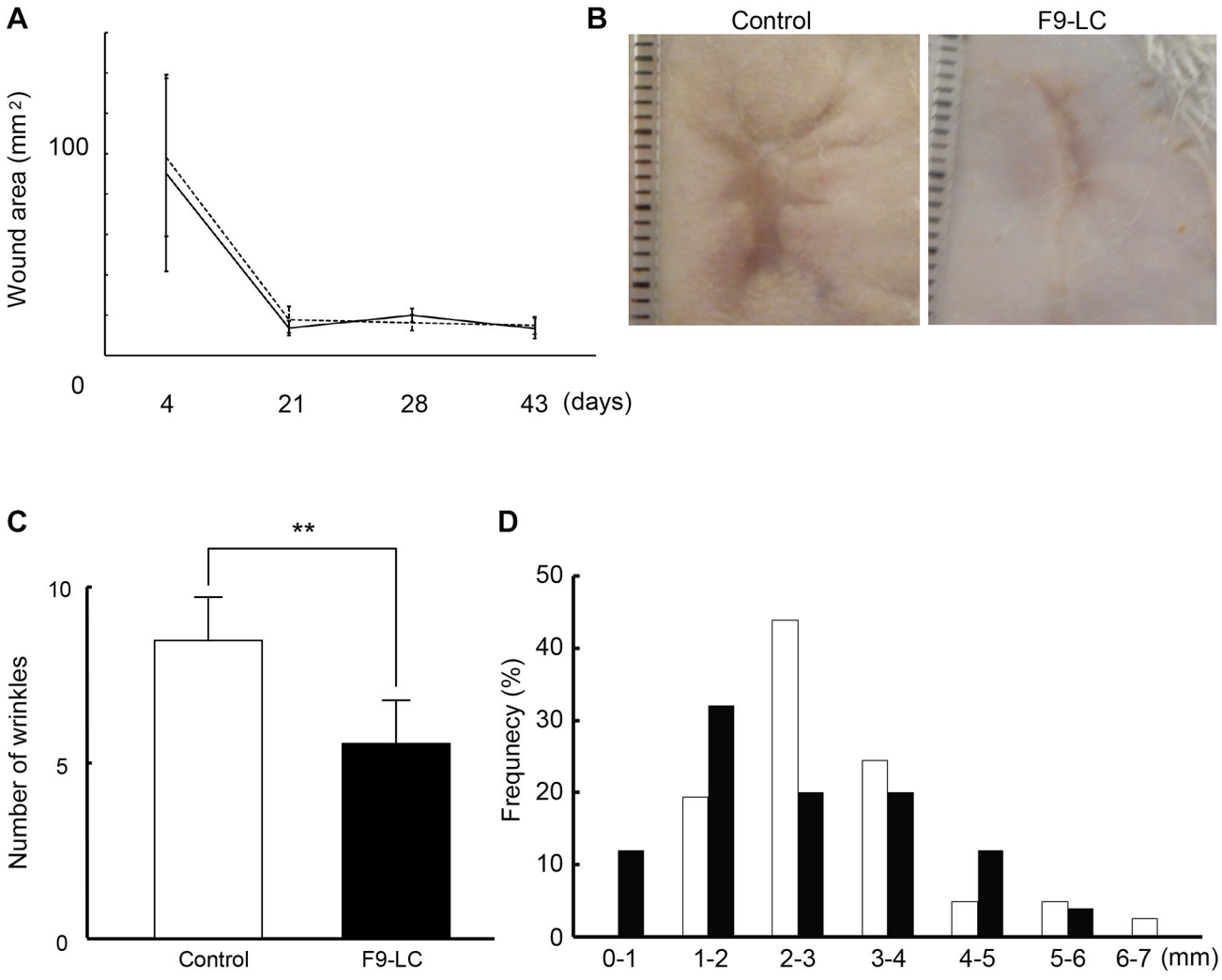

Figure 1. *Macroscopic observation of wounds treated with pAP or pF9-LC. A) Change in denuded area of wounds over time. Solid line, control; dotted line, F9-LC. B) Representative epithelialized wounds. C) Number of wrinkles per wound; n=6. Values are shown as the mean±SD. **p<0.01. D) Histogram of wrinkle length. Open bars, control; closed bars, F9-LC.*

M) OsO_4, embedded in 1% Epon812, and sectioned. Finally, ultrathin sections were stained with saturated uranyl acetate and lead citrate and examined by TEM. PopImaging software (DigitalBeingKid, Kanagawa, Japan) was used to measure the diameter of collagen fibers.

Immunohistochemistry. Rabbit monoclonal anti-collagen 1, collagen 3, α–smooth muscle actin (αSMA), and matrix metalloproteinase-9 (MMP9) (Abcam, Cambridge, MA, USA) were used in this study. Alexa Fluor 488–labeled goat anti-rabbit antibody (Invitrogen) was used as the secondary antibody. Frozen sections were fixed with 4% paraformaldehyde and blocked with 3% albumin in PBS. The sections were then incubated with primary antibody and then with the appropriate secondary antibody. Nuclei were counterstained with Hoechst 33342 (Dojindo, Kumamoto, Japan). Photographs were acquired using a BZ-X700 microscope (Keyence, Osaka, Japan). Fluorescence intensity was measured using Photoshop v 7.0 (Adobe Systems Inc., San Jose, CA, USA). The intensity of control samples was set as 1. Results per view are expressed as mean±standard deviation (SD).

Cell culture. Human skin fibroblasts were purchased from Takara (Kusatsu, Japan) and cultured in fibroblast growth medium (PromoCell, Heidelberg, Germany) lacking serum but containing insulin (5 μg/ml) and basic fibroblast growth factor (1 ng/ml). For morphological examination of fibroblasts, cells were plated on collagen-coated glass-bottom dishes (Matsunami, Osaka, Japan), and recombinant F9-LC protein (1 pM) or control protein (1 pM) was added every day for 8 days. Cells were fixed in 4% paraformaldehyde and permeabilized with 0.1% Triton X-100 for 5 min. Hoechst 33342 (Dojindo) or Sytox (Invitrogen) were used to stain nuclei, and Alexa Fluor 568–labeled phalloidin (Invitrogen) was used to stain actin fibers. Photographs were acquired using a BZ-X700 microscope. For culture on collagen gel, 400 μl of a

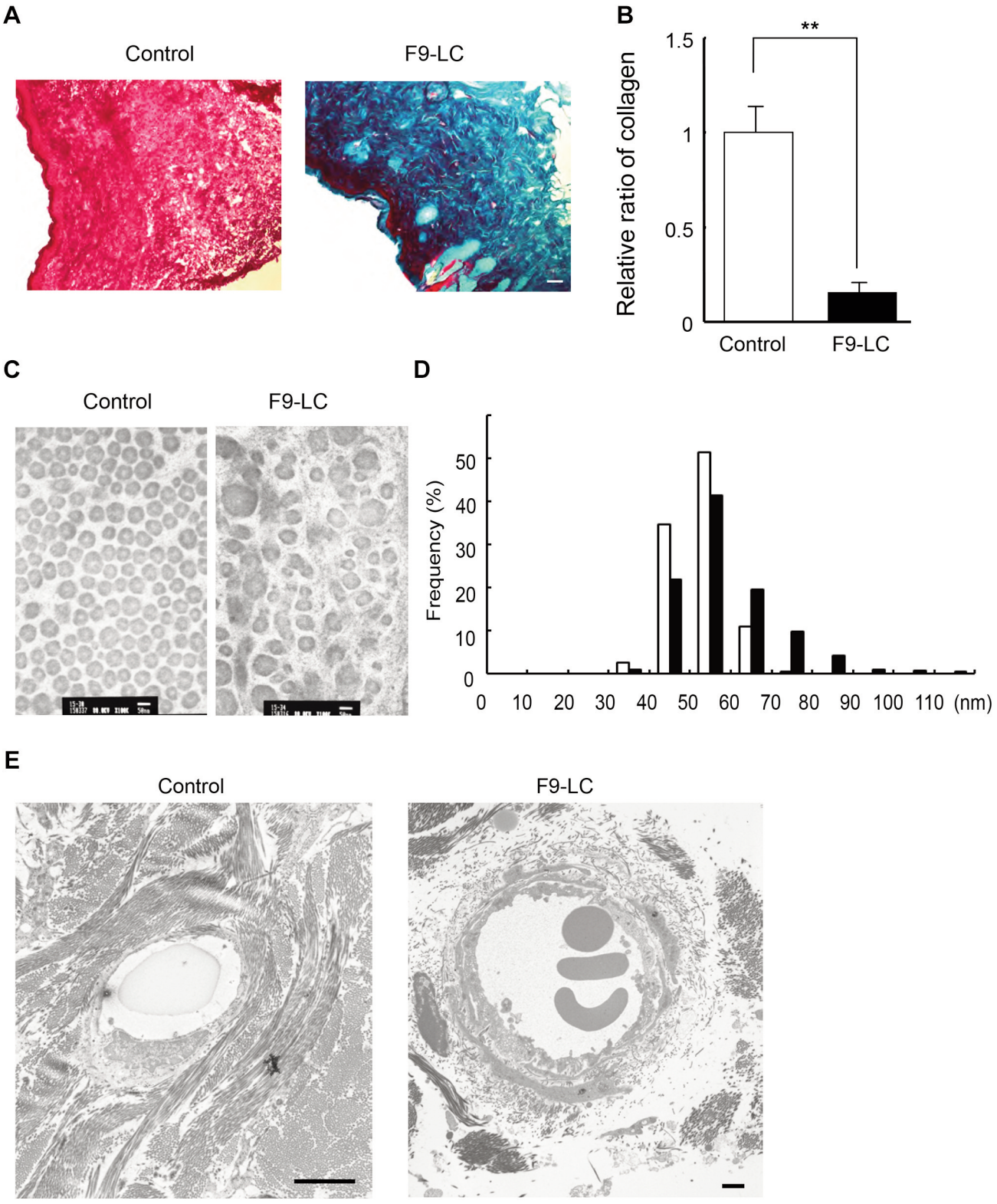

Figure 2. *Collagen in wounds treated with pAP or pF9-LC. A) Collagen staining of wounds. Collagen proteins stained red, and non-collagen proteins stained blue. Scale bar indicates 100 μm. B) Ratio of collagen to non-collagen proteins. Values are indicated as mean±SD. *p<0.01; n=6. C and E) Transmission electron microscopy analysis of collagen fibers in wounds. Scale bars indicate 50 nm. D) Histogram of collagen fiber diameter. Open bars, control; closed bars, F9-LC.*

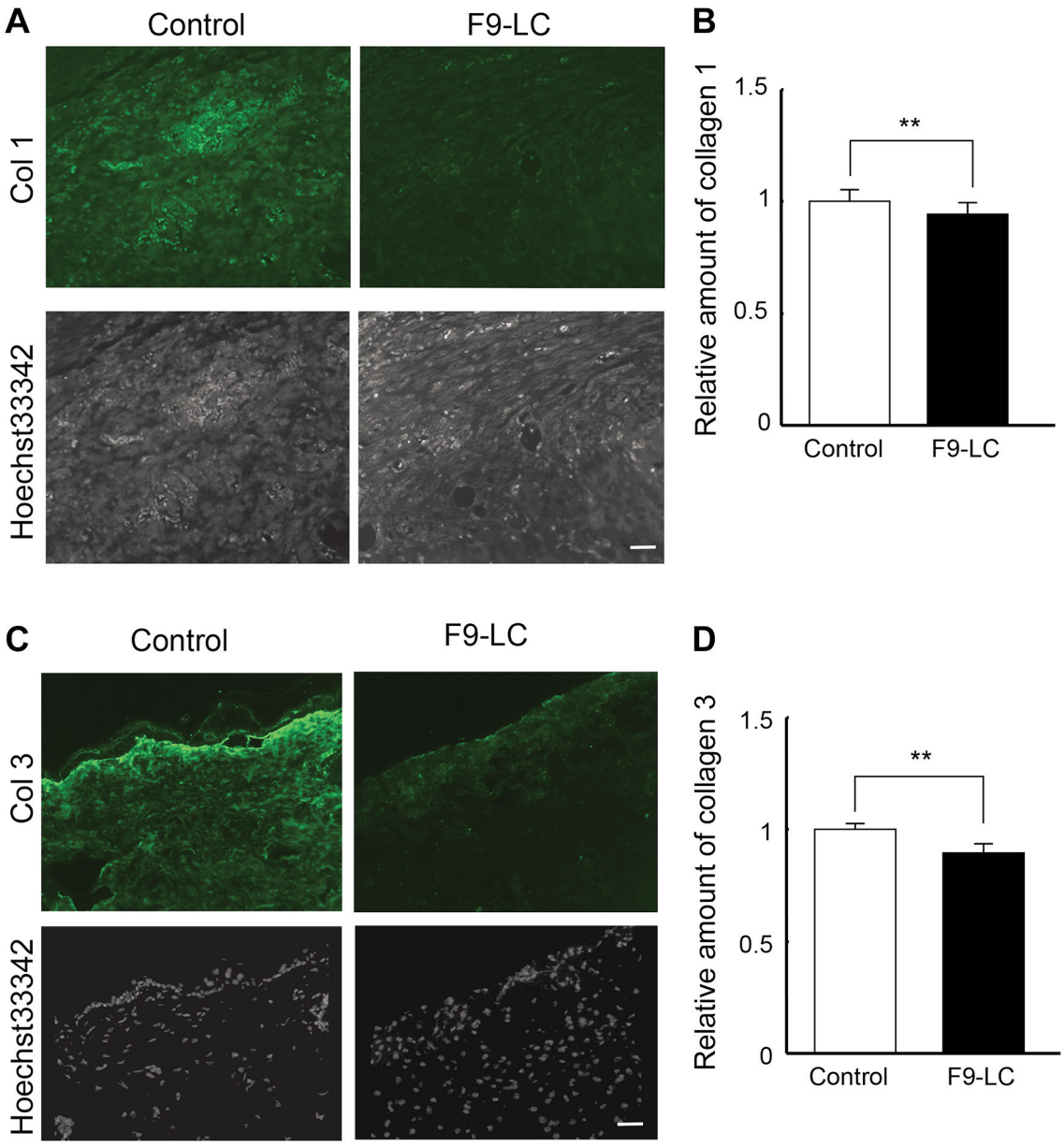

Figure 3. *Immunohistochemistry staining of wounds for collagen type 1 (A) and type 3 (C). Nuclei were stained with Hoechst 33342. Scales bars indicate 100 μm. B, D) Ratio of control to F9-LC. Values are indicated as the mean±SD. **p<0.01; n=8.*

collagen solution, Atelocollagen 2 mg/ml (Koken, Tokyo, Japan), was polymerized in a 24-well dish, and cells were plated on the gel and grown to confluence. Recombinant F9-LC protein (1 pM) or control protein (1 pM) was added every day for 8 days. Cells were then fixed in 4% paraformaldehyde and observed under an SZX-12 objective microscope (Olympus, Tokyo, Japan).

Statistical analysis. Results are expressed as the mean±SD. Data were analyzed in SPSS ver. 27.0.1 (IBM, Armonk, NY, USA) using the Wilcoxon test, as appropriate, and statistical significance was defined as $p<0.05$.

Results

The formation of wrinkles was suppressed by F9-LC treatment. Because gene therapy of tumor-explanted model mice using a Del1 fragment suppressed the growth of cancer parenchyma and stroma, it was expected that forced expression of F9-LC would suppress wound healing. However, macroscopic observation did not indicate any difference between control mice and F9-LC–treated mice during the first few weeks (Figure 1A). However, at 6 weeks,

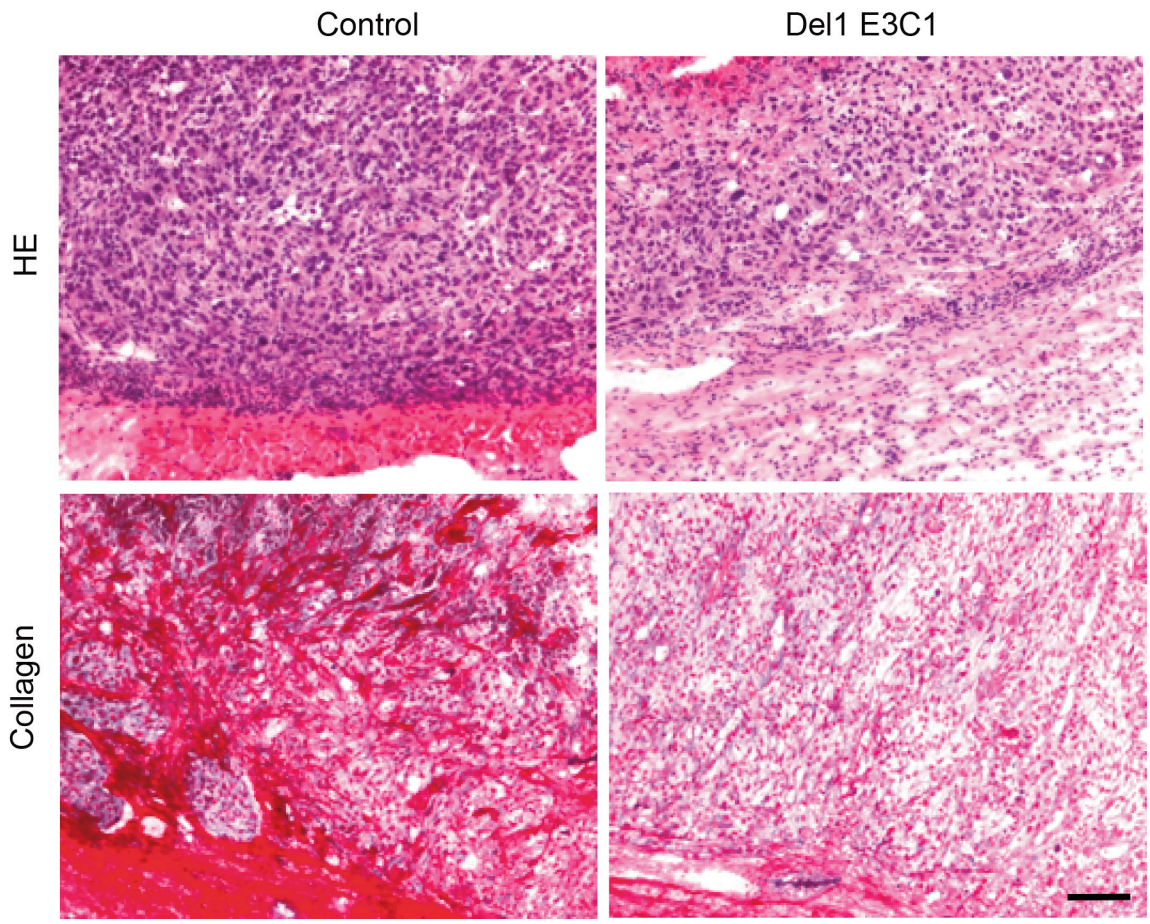

Figure 4. *Explanted tumor treated with Del1 E3C1 fragment. Hematoxylin/eosin (HE) staining or collagen staining of explanted tumor treated with Del1 E3C1 fragment or control protein. Scale bar indicates 100 μm.*

some differences in wound appearance developed between control mice and F9-LC–treated mice (Figure 1B). In control mice, the number of wrinkles was greater than that in F9-LC–treated mice (8.50±1.32 *vs.* 5.57±1.27, control *vs.* F9-LC) ($p<0.01$) (Figure 1C). The frequency of long wrinkles was significantly decreased by F9-LC treatment ($p<0.05$) (Figure 1D). The ratio of wrinkles longer than 2 mm was 80% *versus* 56% (control *vs.* F9-LC) ($p<0.05$).

The morphological characteristics of collagen fibers changed by F9-LC treatment. Because the deposition of collagen proteins causes wound contraction, collagen proteins in wounds were stained (Figure 2A). Collagen proteins were stained red, and non-collagen proteins stained blue. Tissues from control mice stained only red; however, those from F9-LC–treated mice stained blue for the most part. The relative ratio of red to blue was 1.00±0.20 *versus* 0.21±0.09 (control *vs.* F9-LC) ($p<0.01$) (Figure 2B). Next, collagen fibers in wounds were observed under TEM (Figure 2C). Compared with control tissues, the density of collagen fibers in F9-LC–treated tissues was sparse, and the running direction of the fibers was not aligned. Abnormally thick fibers were found in F9-LC–treated tissue, and there was large variation in the diameter of the collagen fibers (Figure 2D). The sparsity of collagen fibers was particularly pronounced around blood vessels (Figure 2E). In addition to the morphological changes in collagen fibers, differences were also observed in blood vessels between control tissues and F9-LC–treated tissues. In F9-LC–treated mice, adhesion between endothelial cells and pericytes was not tight on the basal side, which could explain the edematous spaces in F9-LC–treated tissue. On the luminal side, endothelial cells exhibited protrusions such as microvesicles.

Collagen deposition decreased by F9-LC treatment. Type 1 and type 3 collagen are deposited in wounds. Type 1 collagen is a major protein in healthy skin and healing wounds. The deposition of type 3 collagen increases in the proliferation

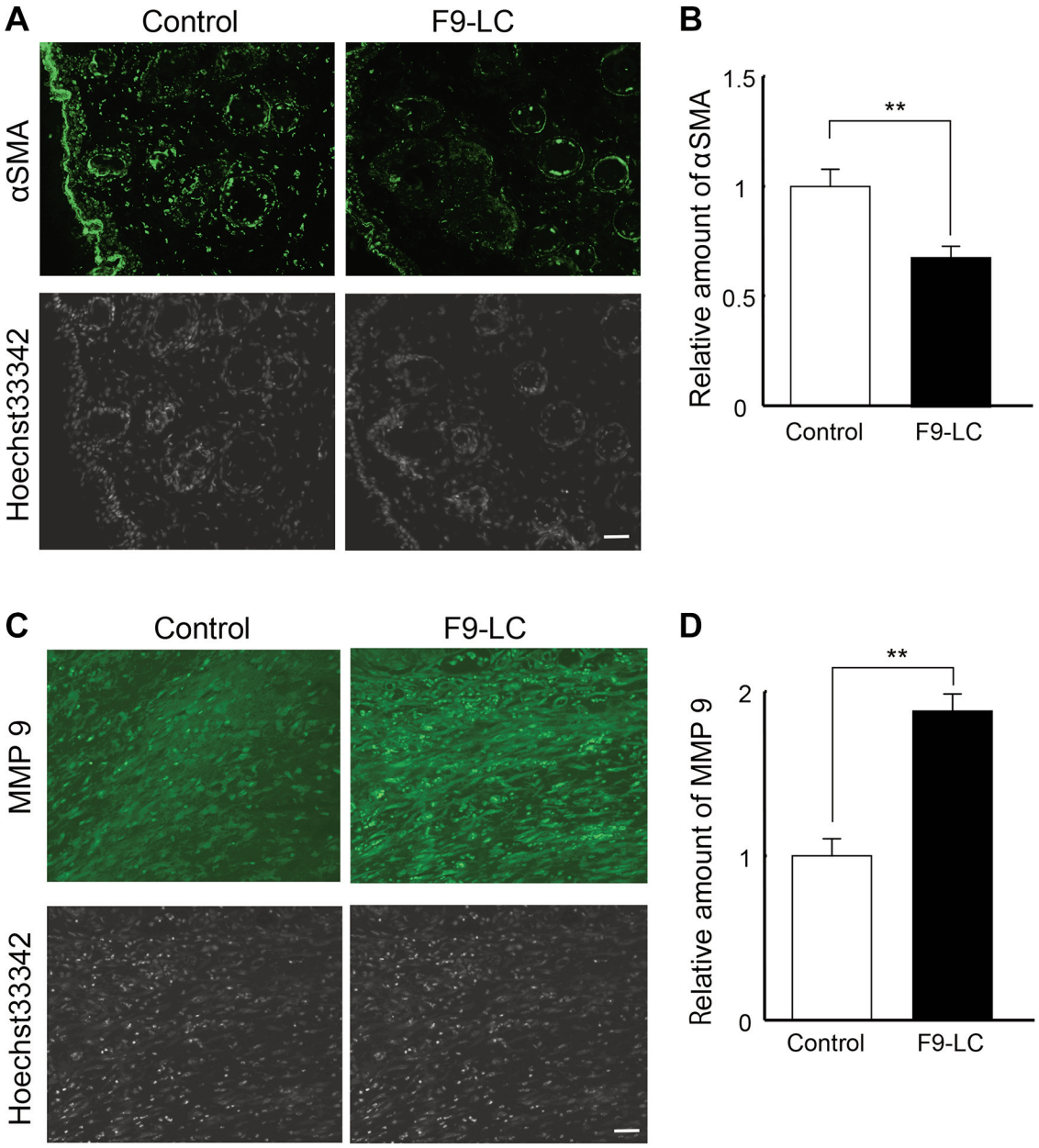

Figure 5. *Immunohistochemistry staining for αSMA and MMP9. Immunohistochemistry staining of wound edge for αSMA (A) or of wound for MMP9 (C). Nuclei were stained with Hoechst 33342. Scales bars indicate 100 μm. B, D) Ratio of control to F9-LC. Values are indicated as the mean±SD. **p<0.01; n=8.*

phase and decreases in the remodeling phase. To evaluate the type of collagen present in healing wounds in this study, immunohistochemistry was performed. In control hypodermal tissue, type 1 collagen was diffusely stained, and forced expression of F9-LC suppressed the deposition of type 1 collagen (Figure 3A). The fluorescence intensity of type 1 collagen was 1.00±0.02 *vs*. 0.94±0.02 (control *vs*. F9-LC) (p<0.01) (Figure 3B). Immunohistochemistry analysis using an anti–type 3 collagen antibody revealed that type 3 collagen was deposited predominantly in the superficial hypodermis, and F9-LC treatment decreased its deposition (Figure 3C). The fluorescence intensity of type 3 collagen was 1.00±0.04 *vs*. 0.89±0.10 (control *vs*. F9-LC) (p<0.01) (Figure 3D).

As discussed previously, a recombinant protein with the EGF motif of Del1 reportedly suppressed the development of cancer stroma in a mouse explanted tumor model. To

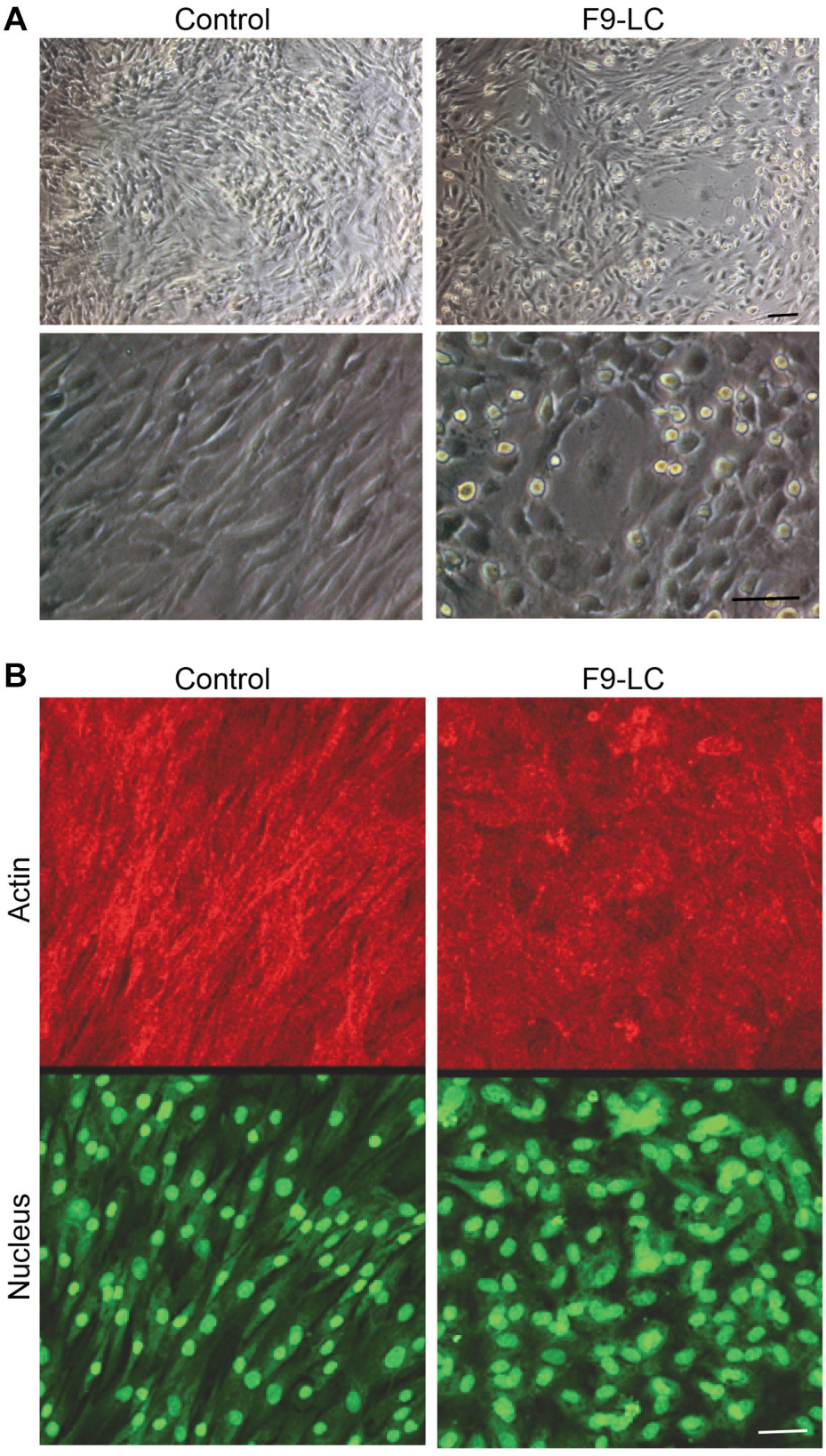

Figure 6. *Continued*

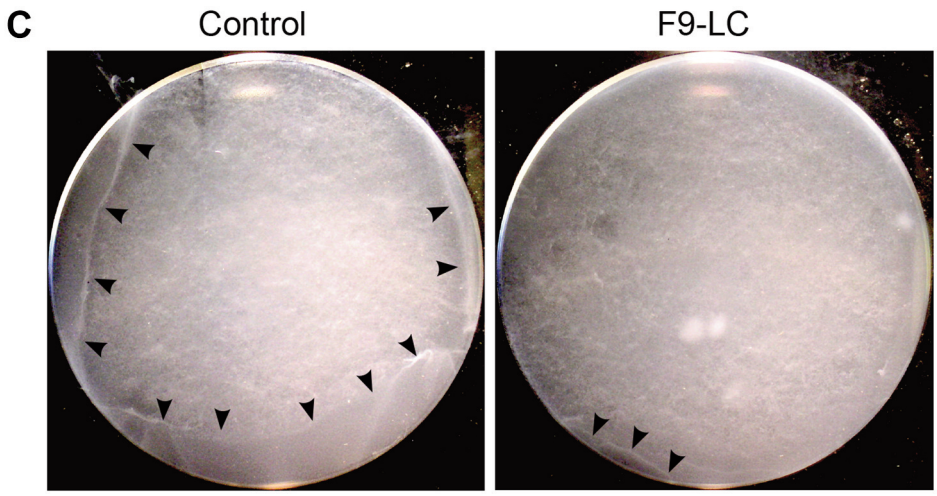

Figure 6. *Effect of F9-LC on fibroblasts in vitro. A) Human dermal fibroblasts were observed under phase contrast microscopy (A) or fluorescence microscopy (B). Cells were cultured on plastic dishes for 8 days with F9-LC or control protein. Scale bars indicate 50 μm. In A, low-magnification view at top and high-magnification view at bottom. In B, fibrous actin was stained with phalloidin conjugated with AlexaFluor 568, and nuclei were stained with Sytox. C) Fibroblasts cultured on collagen gel in a 24-well plate with F9-LC or control protein. Arrowheads indicate the edge of cells detached from the well wall by contraction.*

confirm the functional homology between the EGF motif of Del1 and that of FIX, tumor tissues treated with a recombinant protein with the EGF motif of Del1 were analyzed by collagen staining (Figure 4). Tissues treated with the Del1 fragment exhibited less-positive staining for collagen than control tissues.

The expression of αSMA and MMP9 changed by F9-LC treatment. The expression of proteins related to wound healing were investigated using immunohistochemistry analysis (Figure 5). αSMA is a marker of myofibroblasts that produce collagens and contribute to tissue contraction. The expression of αSMA was decreased around the wounds in F9-LC–treated tissues (Figure 5A). The fluorescence intensity of αSMA was 1.00±0.03 *versus* 0.68±0.02 (control *vs*. F9-LC) ($p<0.01$) (Figure 5B). In the wound healing process, several kinds of MMPs are expressed. MMP9 is a typical gelatinase, and its expression is induced in all phases of wound healing, particularly in the early phase. The expression of MMP9 increased in the hypodermis treated with F9-LC (Figure 5C). The fluorescence intensity of MMP9 was 1.00±0.11 *versus* 1.88±0.13 (control *vs*. F9-LC) ($p<0.01$) (Figure 5D).

Treatment with F9-LC caused morphological changes in cells. Because TEM observations revealed that forced expression of F9-LC resulted in abnormal vessels (Figure 2E), an *in vitro* study using human hypodermal fibroblasts was conducted to determine whether the effects of F9-LC on wound healing represented secondary changes of its effects on blood vessels. Cells were cultured for 8 days with recombinant F9-LC or control protein. In control experiments, cells assumed a spindle form and parallel lines (Figure 6A). Following F9-LC treatment, the cells lost the spindle shape and the orderly line arrangement. Some cells were spherical in shape and others spread extensively. The arrays of actin fibers were examined using phalloidin. In control cells, actin fibers lined in parallel (Figure 6B). However, treatment with F9-LC disrupted this array.

In the *in vivo* study, forced expression of F9-LC attenuated the hubbly surface that occurred in the wound healing process. To determine whether F9-LC decreases the tension around wounds and inhibits contraction by affecting fibroblasts, cells were cultured on collagen gel. Cells were cultured on collagen gel in 24-well dishes for 8 days with recombinant F9-LC or control protein. In control experiments, the cell layer shrank in the wells and detached from the well walls (Figure 6C). Treatment with F9-LC suppressed this phenotype.

Discussion

In the present study, full-thickness wound model mice were prepared, and the effects of forced expression of F9-LC on wound healing were examined. In rats locally injected with cDNA encoding F9-LC, the formation of wrinkles in wounds was suppressed. Collagen deposition and the expression of αSMA were decreased by F9-LC treatment, resulting in the attenuation of fibrosis. In the *in vitro* study using cultured fibroblasts, recombinant F9-LC protein

abolished the typical spindle shape of the cells and the parallel cell arrangement, along with decreased expression of type 1 collagen and αSMA. Because F9-LC treatment exhibited a similar phenotype *in vivo* and *in vitro*, F9-LC appears to directly affect the wound healing process independent of the circulation.

It is thought that F9-LC modulates the wound healing process to produce flat wounds without wrinkles. Wound healing is a long and complex process and begins with hemostasis (hemostasis phase). Platelets release many factors, including transforming growth factor–β1 (TGFβ1), which induces inflammatory cell migration (22). These inflammatory cells produce various cytokines (23). In combination with TGFβ1, these cytokines induce the migration of fibroblasts, epithelial cells, and endothelial cells (24-27). Thrombin and factors of the fibrinolytic system increase vascular permeability (28, 29). These reactions promote progression to the inflammatory phase. In the inflammatory phase, inflammatory cells and MMPs released from fibroblasts and endothelial cells contribute to debridement in the wound (30, 31). The proliferation phase is characterized by cell growth and the accumulation of extracellular matrix, resulting in granulation and scar formation (32). In the proliferation phase, myofibroblasts play important roles, secreting collagen and inducing contraction of the wound (32, 33). TGFβ1 accelerates the differentiation of myofibroblasts and deposition of collagen (34, 35). The remodeling phase continues for one to several years (36, 37). In the remodeling phase, turnover of collagen decreases (38-40), and the generation and degradation of collagen decline (38).

FIX is activated in wounds in the hemostasis phase, and it is thought to play an essential role in the inflammatory phase, as gene targeting of vitamin K–dependent coagulation factors, including FIX, was shown to result in impaired wound healing. Retarded re-epithelialization and reduced inflammatory cell infiltration are found in vitamin K–dependent coagulation factor–knockout mice (41-44). In the present study, the decreased collagen deposition induced by F9-LC treatment suggests that F9-LC plays a role in inflammation or remodeling. TEM observations revealed perivascular edema and microvesicle formation, suggesting inflammation had developed (Figure 2E). The disturbed cell alignment induced by F9-LC in the *in vitro* experiment did not correspond to the phenotype observed in the remodeling phase (Figure 6A and B). It has been reported that a recombinant protein consisting of the EGF domain of FIX accelerates the migration of human umbilical vein endothelial cells (45). In explanted tumors treated with a recombinant protein consisting of the EGF domain from Del1 that contains the CXDXXXXYXCXC sequence, infiltration of CD8-positive lymphocytes is increased (16). Taken together, these data indicate that the forced expression of F9-LC extends the inflammation phase following hemostasis and disrupts progression to the proliferation phase.

The molecular mechanism underlying the effects of EGF has not been well studied. Hidai *et al*. reported that the EGF motif increases the activity of scramblase, causes clustering of lipid rafts, and enhancement of endocytosis (46). Another recent study reported that the EGF motif enhances thrombin-induced intracellular signaling in vascular endothelial cells (47). These data suggest that the EGF motif plays a role in the rapid and strong acute-phase responses of coagulation and inflammation. Further research examining the molecular mechanism of the EGF motif is thus needed.

The EGF motif could be a therapeutic candidate for use in treating fibrosis in other tissues such as the lung, liver, and kidney. Despite the compelling need for therapies for pathological fibrosis, an effective treatment is not available. Kitano *et al*. reported that a recombinant protein with the CXDXXXXYXCXC sequence subcutaneously injected using a non-viral vector inhibited the growth of tumors transplanted in mice (14-17). Their results suggested that the expressed protein was effective not only at the site of subcutaneous injection but also in distant organs.

Conflicts of Interest

There Authors have no conflicts of interest to declare in relation to this study.

Authors' Contributions

Hisataka Kitano, Tomomi Ishikawa performed the research; Hisataka Kitano and Chiaki Hidai designed the research study; Hisataka Kitano, Tomomi Ishikawa, Yoh Masaoka, Kazuhiro Komiyama, and Mamiko Takahashi contributed essential reagents or tools; Hisataka Kitano and Chiaki Hidai wrote the paper.

References

1 Alexanian M, Padmanabhan A, Nishino T, Travers JG, Ye L, Lee CY, Sadagopan N, Huang Y, Pelonero A, Auclair K, Zhu A, Gonzalez Teran B, Flanigan W, Kim CK, Lumbao-Conradson K, Costa M, Jain R, Charo I, Haldar SM, Pollard KS, Vagnozzi RJ, McKinsey TA, Przytycki PF and Srivastava D: Chromatin remodeling drives immune-fibroblast crosstalk in heart failure pathogenesis. bioRxiv, 2023. PMID: 36711864. DOI: 10.1101/2023.01.06.522937

2 Dolivo DM, Sun LS, Rodrigues AE, Galiano RD, Mustoe TA and Hong SJ: Epidermal potentiation of dermal fibrosis: lessons from occlusion and mucosal healing. Am J Pathol, 2023. PMID: 36740181. DOI: 10.1016/j.ajpath.2023.01.008

3 Disphanurat W, Sivapornpan N, Srisantithum B and Leelawattanachai J: Efficacy of a triamcinolone acetonide-loaded dissolving microneedle patch for the treatment of hypertrophic scars and keloids: a randomized, double-blinded, placebo-controlled split-scar study. Arch Dermatol Res, 2022. PMID: 36383222. DOI: 10.1007/s00403-022-02473-6

4 Balachandran A, Choi SB, Beata MM, Małgorzata J, Froemming GRA, Lavilla CA Jr, Billacura MP, Siyumbwa SN and Okechukwu PN: Antioxidant, wound healing potential and in silico assessment of naringin, eicosane and octacosane. Molecules *28(3)*: 1043, 2023. PMID: 36770709. DOI: 10.3390/molecules28031043

5 He C, Zhang W, Tu Y, Zhong L, Wang R, Teng Y, Liao IC and Ding C: Characterization of an ablative fractional CO(2) laser-induced wound-healing model based on *in vitro* 3D reconstructed skin. J Cosmet Dermatol, 2023. PMID: 36683276. DOI: 10.1111/jocd.15597

6 Wang L, Hussain Z, Zheng P, Zhang Y, Cao Y, Gao T, Zhang Z, Zhang Y and Pei R: A mace-like heterostructural enriched injectable hydrogel composite for on-demand promotion of diabetic wound healing. J Mater Chem B *11(10)*: 2166-2183, 2023. PMID: 36779476. DOI: 10.1039/d2tb02403a

7 Uchida DT and Bruschi ML: 3D Printing as a Technological Strategy for the Personalized Treatment of Wound Healing. AAPS PharmSciTech *24(1)*: 41, 2023. PMID: 36698047. DOI: 10.1208/s12249-023-02503-0

8 Zakeri A, Khaseb S, Akhavan Rahnama M, Hajaliaskari A and Soufi Zomorrod M: Exosomes derived from mesenchymal stem cells: A promising cell-free therapeutic tool for cutaneous wound healing. Biochimie *209*: 73-84, 2023. PMID: 36681232. DOI: 10.1016/j.biochi.2023.01.013

9 Aoki M, Matsumoto NM, Dohi T, Kuwahawa H, Akaishi S, Okubo Y, Ogawa R, Yamamoto H and Takabe K: Direct delivery of apatite nanoparticle-encapsulated siRNA targeting TIMP-1 for intractable abnormal scars. Mol Ther Nucleic Acids *22*: 50-61, 2020. PMID: 32911344. DOI: 10.1016/j.omtn.2020.08.005

10 Gobin AS, Rhea R, Newman RA and Mathur AB: Silk-fibroin-coated liposomes for long-term and targeted drug delivery. Int J Nanomedicine *1(1)*: 81-87, 2006. PMID: 17722265. DOI: 10.2147/nano.2006.1.1.81

11 Lazennec G and Lam PY: Recent discoveries concerning the tumor - mesenchymal stem cell interactions. Biochim Biophys Acta *1866(2)*: 290-299, 2016. PMID: 27750042. DOI: 10.1016/j.bbcan.2016.10.004

12 Akita S, Akino K, Imaizumi T, Tanaka K, Anraku K, Yano H and Hirano A: The quality of pediatric burn scars is improved by early administration of basic fibroblast growth factor. J Burn Care Res *27(3)*: 333-338, 2006. PMID: 16679903. DOI: 10.1097/01.BCR.0000216742.23127.7A

13 Bougnaud S, Golebiewska A, Oudin A, Keunen O, Harter PN, Mäder L, Azuaje F, Fritah S, Stieber D, Kaoma T, Vallar L, Brons NH, Daubon T, Miletic H, Sundstrøm T, Herold-Mende C, Mittelbronn M, Bjerkvig R and Niclou SP: Molecular crosstalk between tumour and brain parenchyma instructs histopathological features in glioblastoma. Oncotarget *7(22)*: 31955-31971, 2016. PMID: 27049916. DOI: 10.18632/oncotarget.7454

14 Kitano H, Masaoka Y, Mamiya A, Fujiwara Y, Miki T and Hidai C: Combination cancer therapy of a Del1 fragment and cisplatin enhanced therapeutic efficiency *in vivo*. In Vivo *35(2)*: 779-791, 2021. PMID: 33622870. DOI: 10.21873/invivo.12318

15 Kitano H, Mamiya A, Ishikawa T, Fujiwara Y, Masaoka Y, Miki T and Hidai C: An epidermal growth factor motif of developmental endothelial locus 1 protein inhibits efficient angiogenesis in explanted squamous cell carcinoma *in vivo*. Rev Invest Clin *73(1)*: 039-051, 2020. PMID: 33052897. DOI: 10.24875/RIC.20000375

16 Kitano H, Ishikawa T, Tamura E, Kokubun S and Hidai C: Efficient cancer gene therapy with a Del1 fragment administered by hypodermic injection in a mouse explanted tumor model. Translational Cancer Research *7(3)*: 686-694, 2018. DOI: 10.21037/tcr.2018.05.45

17 Kitano H, Mamiya A, Ishikawa T, Egoshi K, Kokubun S and Hidai C: Long-term gene therapy with Del1 fragment using nonviral vectors in mice with explanted tumors. Onco Targets Ther *9*: 503-516, 2016. PMID: 26889088. DOI: 10.2147/OTT.S90801

18 Kitano H, Mamiya A, Kokubun S and Hidai C: Efficient nonviral gene therapy with FasL and Del1 fragments in mice. J Gene Med *14(11)*: 642-650, 2012. PMID: 23136083. DOI: 10.1002/jgm.2682

19 Kitano H, Kokubun S and Hidai C: The extracellular matrix protein Del1 induces apoptosis *via* its epidermal growth factor motif. Biochem Biophys Res Commun *393(4)*: 757-761, 2010. PMID: 20171188. DOI: 10.1016/j.bbrc.2010.02.076

20 Stojanovski BM and Di Cera E: Comparative sequence analysis of vitamin K-dependent coagulation factors. J Thromb Haemost *20(12)*: 2837-2849, 2022. PMID: 36156849. DOI: 10.1111/jth.15897

21 Hidai C: EGF-like domains with a C-x-D-x(4)-Y-x-C motif. Open Access Journal of Translational Medicine & Research *2(2)*: 67-71, 2022. DOI: 10.15406/oajtmr.2018.02.00039

22 Hotta E, Tamagawa-Mineoka R and Katoh N: Platelets are important for the development of immune tolerance: Possible involvement of TGF-β in the mechanism. Exp Dermatol *28(7)*: 801-808, 2019. PMID: 30991458. DOI: 10.1111/exd.13940

23 Tu W, Xiao X, Lu J, Liu X, Wang E, Yuan R, Wan R, Shen Y, Xu D, Yang P, Gong M, Gao P and Huang SK: Vanadium exposure exacerbates allergic airway inflammation and remodeling through triggering reactive oxidative stress. Front Immunol *13*: 1099509, 2023. PMID: 36776398. DOI: 10.3389/fimmu.2022.1099509

24 Kimura Y, Fujimori M, Rajagopalan NR, Poudel K, Kim K, Nagar K, Vroomen LG, Reis H, Al-Ahmadie H, Coleman JA and Srimathveeravalli G: Macrophage activity at the site of tumor ablation can promote murine urothelial cancer *via* transforming growth factor-β1. Front Immunol *14*: 1070196, 2023. PMID: 36761730. DOI: 10.3389/fimmu.2023.1070196

25 Wang R, Bhatt AB, Minden-Birkenmaier BA, Travis OK, Tiwari S, Jia H, Rosikiewicz W, Martinot O, Childs E, Loesch R, Tossou G, Jamieson S, Finkelstein D, Xu B and Labelle M: ZBTB18 restricts chromatin accessibility and prevents transcriptional adaptations that drive metastasis. Sci Adv *9(1)*: eabq3951, 2023. PMID: 36608120. DOI: 10.1126/sciadv.abq3951

26 Ungefroren H, Braun R, Lapshyna O, Konukiewitz B, Wellner UF, Lehnert H and Marquardt JU: Suppressive role of ACVR1/ALK2 in basal and TGFβ1-induced cell migration in pancreatic ductal adenocarcinoma cells and identification of a self-perpetuating autoregulatory loop involving the small GTPase RAC1b. Biomedicines *10(10)*: 2640, 2022. PMID: 36289908. DOI: 10.3390/biomedicines10102640

27 Elmansi AM, Eisa NH, Periyasamy-Thandavan S, Kondrikova G, Kondrikov D, Calkins MM, Aguilar-Pérez A, Chen J, Johnson M, Shi XM, Reitman C, McGee-Lawrence ME, Crawford KS, Dwinell MB, Volkman BF, Blumer JB, Luttrell LM, McCorvy JD and Hill WD: DPP4-truncated CXCL12 alters CXCR4/ACKR3

signaling, osteogenic cell differentiation, migration, and senescence. ACS Pharmacol Transl Sci *6(1)*: 22-39, 2022. PMID: 36659961. DOI: 10.1021/acsptsci.2c00040

28 Rahmani F, Abdeahad H, Jaberi N, Hanaie R, Soleimani A, Avan A, Khazaei M and Hassanian SM: The protective effect of curcumin on thrombin-induced hyper-permeability. Avicenna J Phytomed *13(1)*: 97-108, 2023. PMID: 36698738. DOI: 10.22038/AJP.2022.21025

29 Murugesan N, Üstunkaya T and Feener EP: Thrombosis and hemorrhage in diabetic retinopathy: a perspective from an inflammatory standpoint. Semin Thromb Hemost *41(6)*: 659-664, 2015. PMID: 26305236. DOI: 10.1055/s-0035-1556731

30 Sugioka K, Mishima H, Kodama A, Itahashi M, Fukuda M and Shimomura Y: Regulatory mechanism of collagen degradation by keratocytes and corneal inflammation: the role of urokinase-type plasminogen activator. Cornea *35 Suppl 1*: S59-S64, 2016. PMID: 27661072. DOI: 10.1097/ICO.0000000000000995

31 Utz ER, Elster EA, Tadaki DK, Gage F, Perdue PW, Forsberg JA, Stojadinovic A, Hawksworth JS and Brown TS: Metalloproteinase expression is associated with traumatic wound failure. J Surg Res *159(2)*: 633-639, 2010. PMID: 20056248. DOI: 10.1016/j.jss.2009.08.021

32 Reinke JM and Sorg H: Wound repair and regeneration. Eur Surg Res *49(1)*: 35-43, 2012. PMID: 22797712. DOI: 10.1159/000339613

33 Pattarayan D, Sivanantham A, Bethunaickan R, Palanichamy R and Rajasekaran S: Tannic acid modulates fibroblast proliferation and differentiation in response to pro-fibrotic stimuli. J Cell Biochem *119(8)*: 6732-6742, 2018. PMID: 29665059. DOI: 10.1002/jcb.26866

34 Ragazzini S, Scocozza F, Bernava G, Auricchio F, Colombo GI, Barbuto M, Conti M, Pesce M and Garoffolo G: Mechanosensor YAP cooperates with TGF-β1 signaling to promote myofibroblast activation and matrix stiffening in a 3D model of human cardiac fibrosis. Acta Biomater *152*: 300-312, 2022. PMID: 36055606. DOI: 10.1016/j.actbio.2022.08.063

35 Ju N, Hayashi H, Shimamura M, Baba S, Yoshida S, Morishita R, Rakugi H and Nakagami H: Prevention of bleomycin-induced pulmonary fibrosis by a RANKL peptide in mice. Sci Rep *12(1)*: 12474, 2022. PMID: 35864207. DOI: 10.1038/s41598-022-16843-7

36 Lyu K, Liu X, Jiang L, Chen Y, Lu J, Zhu B, Liu X, Li Y, Wang D and Li S: The functions and mechanisms of low-level laser therapy in tendon repair (review). Front Physiol *13*: 808374, 2022. PMID: 35242050. DOI: 10.3389/fphys.2022.808374

37 Gurtner GC, Werner S, Barrandon Y and Longaker MT: Wound repair and regeneration. Nature *453(7193)*: 314-321, 2008. PMID: 18480812. DOI: 10.1038/nature07039

38 Diller RB and Tabor AJ: The role of the extracellular matrix (ECM) in wound healing: a review. Biomimetics (Basel) *7(3)*: 87, 2022. PMID: 35892357. DOI: 10.3390/biomimetics7030087

39 Lee YI, Lee SG, Kim J, Choi S, Jung I and Lee JH: Proteoglycan combined with hyaluronic acid and hydrolyzed collagen restores the skin barrier in mild atopic dermatitis and dry, eczema-prone skin: a pilot study. Int J Mol Sci *22(19)*: 10189, 2021. PMID: 34638528. DOI: 10.3390/ijms221910189

40 Ferrara PJ, Reidy PT, Petrocelli JJ, Yee EM, Fix DK, Mahmassani ZS, Montgomery JA, McKenzie AI, de Hart NMMP and Drummond MJ: Global deletion of CCL2 has adverse impacts on recovery of skeletal muscle fiber size and function and is muscle specific. J Appl Physiol (1985) *134(4)*: 923-932, 2023. PMID: 36861669. DOI: 10.1152/japplphysiol.00444.2022

41 Renné T, Pozgajová M, Grüner S, Schuh K, Pauer HU, Burfeind P, Gailani D and Nieswandt B: Defective thrombus formation in mice lacking coagulation factor XII. J Exp Med *202(2)*: 271-281, 2005. PMID: 16009717. DOI: 10.1084/jem.20050664

42 Yanagita M, Ishimoto Y, Arai H, Nagai K, Ito T, Nakano T, Salant DJ, Fukatsu A, Doi T and Kita T: Essential role of Gas6 for glomerular injury in nephrotoxic nephritis. J Clin Invest *110(2)*: 239-246, 2002. PMID: 12122116. DOI: 10.1172/JCI14861

43 Butschkau A, Wagner NM, Bierhansl L, Genz B and Vollmar B: Protein Z-deficiency is associated with enhanced neointima formation and inflammatory response after vascular injury in mice. Int J Clin Exp Pathol *7(9)*: 6064-6071, 2014. PMID: 25337252.

44 Shumilina E, Nurbaeva MK, Yang W, Schmid E, Szteyn K, Russo A, Heise N, Leibrock C, Xuan NT, Faggio C, Kuro-o M and Lang F: Altered regulation of cytosolic Ca^{2+} concentration in dendritic cells from klotho hypomorphic mice. Am J Physiol Cell Physiol *305(1)*: C70-C77, 2013. PMID: 23596175. DOI: 10.1152/ajpcell.00355.2012

45 Mamiya A, Kitano H, Kokubun S and Hidai C: Activation peptide of coagulation factor IX regulates endothelial permeability. Transl Res *177*: 70-84.e5, 2016. PMID: 27392935. DOI: 10.1016/j.trsl.2016.06.006

46 Hidai C, Fujiwara Y, Kokubun S and Kitano H: EGF domain of coagulation factor IX is conducive to exposure of phosphatidylserine. Cell Biol Int *41(4)*: 374-383, 2017. PMID: 28150893. DOI: 10.1002/cbin.10733

47 Tamura E, Kitano H, Mamiya A, Kokubun S and Hidai C: The first EGF domain of coagulation factor IX increases PAR1 distributionin lipid rafts and modulates the response to thrombin in endothelial cells. Journal of Nihon University Medical Association *81(6)*: 355-365, 2023. DOI: 10.4264/numa.81.6_355

Received March 28, 2023
Revised April 8, 2023
Accepted April 10, 2023